Analytical Analysis of the Impact of RF Circuits on the Optimal Trade-Off Between Energy Efficiency and Spectral Efficiency in Fifth-Generation Small Cell Networks

Mohamad Younes and Yves Louet

Abstract – This article presents an analytical solution aimed at optimizing the trade-off between energy efficiency (EE) and spectral efficiency (SE) within small cell fifth-generation communication systems. This approach includes energy consumption modeling, encompassing both power amplifier and RF circuits. We evaluate two distinct models for quantifying the energy consumption of RF circuits: the first being a static energy consumption (SEC) model, while the second is a static and dynamic energy consumption (SDEC) model. The central objective of this article is to thoroughly analyze how the static and dynamic components of these two models, as well as the system parameters, influence the optimal trade-off between EE and SE. Note that the formulation of the EE problem as a function of SE has a convex characteristic, allowing an optimal solution both numerically and analytically to be found. Detailed comparisons, carried out under various conditions, highlight the high accuracy of this analytical solution compared with the optimal numerical solution, whether using the SEC model or the SDEC model. In addition, note that our model, although based on a generic emitter–receiver structure, proves flexible enough to be used in the analysis of other communication architectures.

1. Introduction

In recent years, the increasing adoption of small cell base stations (BSs) for future generations of telecommunications, notably fifth generation (5G) and sixth generation (6G), has become a dominant trend due to potential advantages, such as improved data rates and cell coverage compared with previous generations, such as fourth generation [1, 2]. Small cell BSs, characterized by compact size, offer great flexibility for deployment, making them particularly suitable for densely populated areas or environments in which the implementation of traditional telecom infrastructure is hampered by physical or regulatory constraints [3]. However, note that the need for a large number of small cell BSs to meet the requirements of 5G communications results in considerable energy consumption, raising concerns about the environmental impact. Consequently, it becomes imperative to look for ways to optimize the energy consumption of these BSs to reduce the environmental footprint, while maintaining communication quality of service (QoS) [3, 4].

The crucial issue of reconciling energy consumption and QoS was the subject of much previous research [3, 5–7]. However, note that these studies mainly focused on traditional networks, characterized by macro cells covering long distances, thus emphasizing the optimization of transmission-related energy consumption. In contrast, with the emergence of future mobile networks based on small cells, BSs are deployed in close proximity to each other, implying generally shorter transmission distances. This configuration leads to a major peculiarity: when these small cell BSs are deployed in large numbers, the energy consumed by the baseband units to process traffic can be comparable to, or even greater than, that used for the transmission itself.

This article focuses on optimizing the trade-off between energy efficiency (EE) and spectral efficiency (SE) in small cell 5G and 6G networks. This optimization is not solely limited to the energy consumed by transmission but also includes the energy associated with computations performed by RF circuits. This study builds on a previous article [8]; we addressed this issue by proposing a numerical optimization on the basis of Shannon's capacity. We extend those investigations by examining the impact of two distinct models for quantifying the energy consumption of RF circuits. The first model, known as the static energy consumption (SEC) model, is widely used because of its simplicity; it assumes that RF circuit power remains constant. By contrast, the second model, known as the static and dynamic energy consumption (SDEC) model, breaks this power down into two components: a constant and a variable, with the latter being linearly dependent on bandwidth. Note that the SDEC model proves particularly suitable for analyzing the energy consumption associated with analog-to-digital and digital-to-analog converters, as reported in [9]. In addition, the SDEC model proves effective in baseband signal processing, encompassing essential functions such as modulation, demodulation, equalization, filtering, predistortion, and many other operations.

Our approach to optimize the trade-off between EE and SE is based on a fundamental feature of the problem: the intrinsically convex variation of EE as a

Manuscript received 12 November 2023.

Mohamad Younes is with the Research Center of the Military Academy of Saint-Cyr Coëtquidan, Guer 56381, France; e-mail: mohamad.younes@st-cyr.terre-net.defense.gouv.fr.

Yves Louet is with the IETR UMR CNRS 6164, CentraleSupélec at Rennes Campus, Cesson-Sévigné 35557, France; e-mail: yves.louet@centralesupelec.fr.

function of SE. This property offers both numerically and analytically the possibility of determining an optimal solution to the trade-off, whatever the RF circuit energy consumption model under consideration. To this end, this article focuses on solving this challenge by proposing an analytical solution for determining optimal EE and SE values. Comparisons demonstrate the high accuracy of this analytical solution compared with the optimal numerical solution that applies to the SEC and SDEC models. However, for a deeper understanding of the robustness of the trade-off to parameter variations [10–12], it is essential to assess the sensitivity of the optimal point. To address these challenges, this article also looks at the analytical evaluation of the robustness of the optimal trade-off in response to variations in the values of the constant and dynamic components associated with the SEC and SDEC models. This detailed approach allows in-depth exploration of the dynamics of energy consumption in RF circuits, highlighting aspects crucial to overall system efficiency.

2. Trade-Off Between EE and SE

The channel is modeled according to the 3rd Generation Partnership Project (3GPP) specifications [13], where the power received P_r (watts) by a user at a distance d (meters) from the BS is calculated by using the formula $P_r = P_t \frac{G_t G_r k}{d^\alpha}$, where P_t is the transmission power of the BS (watts), α is the path loss exponent, G_t and G_r represent the gains of the transmitting and receiving antennas, respectively, and k is the attenuation coefficient at 1 m. Noise power P_N (watts) is determined as a function of Boltzmann's constant K (joule per kelvin), receiver system temperature T (kelvin), and bandwidth B (hertz): $P_N = KTB$. Thus, the signal-to-noise ratio (SNR) is given by

$$\mathrm{SNR} = \frac{P_r}{P_N} = P_t \frac{G_t G_r k}{KTBd^\alpha} \tag{1}$$

Using the equations defining SE as $\mathrm{SE} = \frac{R}{B}$ (bits per second per hertz) and EE per bit as $\mathrm{EE}_b = \frac{R}{P_t}$ (bit per joule), where R represents the bit rate (bit per second), we can express SNR as follows:

$$\mathrm{SNR} = \frac{R}{\mathrm{EE}_b} \frac{G_t G_r k}{KTBd^\alpha} = \frac{1}{\mathrm{EE}_b} \mathrm{SE} \frac{G_t G_r k}{KTd^\alpha} \tag{2}$$

Thus, to guarantee QoS in line with the service provider's requirements, the capacity of a communication system (C), defined as $C = B\log_2(1 + \mathrm{SNR})$, must be chosen to meet the following condition $C = B\log_2\left(1 + \frac{1}{\mathrm{EE}_b} \mathrm{SE} \frac{G_t G_r k}{KTd^\alpha}\right) \geq R$. Consequently, the maximum EE per bit $\mathrm{EE}_{b,\max}$ (bit per joule) is expressed as follows:

$$\mathrm{EE}_{b,\max} = \frac{G_t G_r k}{KTd^\alpha} \frac{\mathrm{SE}}{2^{\mathrm{SE}} - 1} \tag{3}$$

On the other hand, the minimum energy per transmitted bit ($E_{b,\min}$), defined as the inverse of $\mathrm{EE}_{b,\max}$ expressed in (3) [14], is as follows: $E_{b,\min} = \frac{1}{\mathrm{EE}_{b,\max}} = \frac{KTd^\alpha}{G_t G_r k} \frac{2^{\mathrm{SE}} - 1}{\mathrm{SE}}$ (joule per bit). In traditional long-distance networks, this energy is mainly associated with transmission. However, in the context of short-range 5G networks, the energy consumption of RF circuits can become predominant. Consequently, it becomes imperative to reach an optimal trade-off between SE and EE, considering the specific characteristics of the system, notably, the energy consumption of the power amplifier and RF circuits. In this context, the total power consumed $P_{t,\mathrm{tot}}$ (watts) is made up of the power amplifier power P_{pa} (watts) and the RF circuit power P_{cir} (watts), that is, $P_{t,\mathrm{tot}} = P_{\mathrm{pa}} + P_{\mathrm{cir}}$. In general, P_{pa} is estimated as a function of amplifier efficiency (η_{PA}) as follows: $P_{\mathrm{pa}} = \frac{1}{\eta_{\mathrm{PA}}} P_t$. Consequently, the total energy consumed $E_{b,\mathrm{tot}}$ (joule per bit) is the sum of the energy consumed in transmission (E'_b) and the energy dedicated to RF circuits (E_{cir}):

$$E_{b,\mathrm{tot}} = \frac{P_{t,\mathrm{tot}}}{R} = E'_b + E_{\mathrm{cir}} \tag{4}$$

with

$$E'_b = \frac{1}{\eta_{\mathrm{PA}}} E_{b,\min} = \frac{1}{\eta_{\mathrm{PA}}} \frac{KTd^\alpha}{G_t G_r k} \frac{2^{\mathrm{SE}} - 1}{\mathrm{SE}} \tag{5}$$

We explore the modeling of RF circuit energy consumption using two distinct models, namely, the SEC model and the SDEC model. The SEC model maintains RF circuit power (P_{cir}) at a fixed value, denoted $P_{\mathrm{cir}} = P_c$, while the SDEC model decomposes P_{cir} into two distinct components: a constant part (P_c) and a part linearly dependent on B, denoted $P_{\mathrm{cir}} = P_c + \gamma B$. The parameter γ is directly related to the complexity of the processing operations performed by the circuits. Consequently, the energy consumed by the circuits in the SDEC model is defined as follows:

$$E_{\mathrm{cir}} = \frac{P_{\mathrm{cir}}}{\mathrm{SE}.B} = \frac{P_c + \gamma B}{\mathrm{SE}.B} = \left(\frac{P_c}{B} + \gamma\right) \frac{1}{\mathrm{SE}} \tag{6}$$

Thus, in the SDEC model, EE is the inverse of $E_{b,\mathrm{tot}}$ and is expressed as follows:

$$\mathrm{EE} = \frac{1}{E_{b,\mathrm{tot}}} = \frac{\mathrm{SE}}{\frac{1}{\eta_{\mathrm{PA}}} \frac{KTd^\alpha}{G_t G_r k} (2^{\mathrm{SE}} - 1) + \left(\frac{P_c}{B} + \gamma\right)} \tag{7}$$

Finally, note that in the SEC model, EE is obtained by taking $\gamma = 0$.

3. Analytical Optimization of EE and SE with SEC and SDEC models

When P_{cir} is nonzero in the SEC and SDEC models, EE exhibits a convex characteristic with respect to SE, with a global maximum in $(\text{SE}^*, \text{EE}^*)$. This notion is clearly illustrated in the following section, notably through Figure 1, which graphically shows the evolution of EE as a function of SE. Note that SE^* represents the optimal SE aimed at minimizing total energy consumption ($E^*_{b,\text{tot}}$) or, in other words, maximizing EE. To determine SE^*, simply solve $\frac{d}{d\text{SE}}\text{EE} = 0$ using the EE expression formulated in (7). Applying the property $2^{\text{SE}} = e^{\text{SE}.\ln(2)}$, we obtain

$$\begin{aligned}\frac{d}{d\text{SE}}\text{EE} = &\left(\frac{1}{\eta_{\text{PA}}}\frac{KTd^{\alpha}}{G_tG_rk}(2^{\text{SE}^*}-1)+\left(\frac{P_c}{B}+\gamma\right)\right)^{-1}\\ &+\text{SE}^*(-1)\left(\frac{1}{\eta_{\text{PA}}}\frac{KTd^{\alpha}}{G_tG_rk}\left(\ln(2)e^{\text{SE}^*.\ln(2)}\right)\right).\\ &\left(\frac{1}{\eta_{\text{PA}}}\frac{KTd^{\alpha}}{G_tG_rk}(2^{\text{SE}^*}-1)+\left(\frac{P_c}{B}+\gamma\right)\right)^{-2}\\ =&\ 0\end{aligned} \tag{8}$$

Dividing (8) by $\left(\frac{1}{\eta_{\text{PA}}}\frac{KTd^{\alpha}}{G_tG_rk}(2^{\text{SE}^*}-1)+\left(\frac{P_c}{B}+\gamma\right)\right)^{-2} \neq 0$, we find

$$\begin{aligned}&\frac{1}{\eta_{\text{PA}}}\frac{KTd^{\alpha}}{G_tG_rk}(2^{\text{SE}^*}-1)+\left(\frac{P_c}{B}+\gamma\right)\\ &=\text{SE}^*\left(\frac{1}{\eta_{\text{PA}}}\frac{KTd^{\alpha}}{G_tG_rk}\left(\ln(2)e^{\text{SE}^*.\ln(2)}\right)\right)\end{aligned} \tag{9}$$

Now dividing (9) by $\frac{1}{\eta_{\text{PA}}}\frac{KTd^{\alpha}}{G_tG_rk}$, we obtain

$$(2^{\text{SE}^*}-1)+\frac{\left(\frac{P_c}{B}+\gamma\right)}{\frac{1}{\eta_{\text{PA}}}\frac{KTd^{\alpha}}{G_tG_rk}}=\text{SE}^*\left(\ln(2)e^{\text{SE}^*.\ln(2)}\right) \tag{10}$$

By grouping the SE^*-dependent terms, we can express (10) as follows:

$$\begin{aligned}&\text{SE}^*\left(\ln(2)e^{\text{SE}^*.\ln(2)}\right)-2^{\text{SE}^*}=\frac{\left(\frac{P_c}{B}+\gamma\right)}{\frac{1}{\eta_{\text{PA}}}\frac{KTd^{\alpha}}{G_tG_rk}}-1\\ &\Rightarrow e^{\text{SE}^*.\ln(2)}(\text{SE}^*.\ln(2)-1)=\frac{\left(\frac{P_c}{B}+\gamma\right)}{\frac{1}{\eta_{\text{PA}}}\frac{KTd^{\alpha}}{G_tG_rk}}-1\end{aligned} \tag{11}$$

Using the property of Lambert's function W such that $e^{\varpi}\varpi = z \iff \varpi = W(z)$, we can write

$$\begin{aligned}&e^{\text{SE}^*.\ln(2)-1}(\text{SE}^*.\ln(2)-1)=\frac{\left(\frac{P_c}{B}+\gamma\right)}{e\frac{1}{\eta_{\text{PA}}}\frac{KTd^{\alpha}}{G_tG_rk}}-e^{-1}\\ &\Rightarrow \text{SE}^*.\ln(2)-1=W\left(\frac{\left(\frac{P_c}{B}+\gamma\right)\eta_{\text{PA}}G_tG_rk}{eKTd^{\alpha}}-e^{-1}\right)\end{aligned} \tag{12}$$

Thus, the optimal values of SE and EE in the SDEC model are expressed as follows:

$$\text{SE}^*=\frac{W\left(\frac{\left(\frac{P_c}{B}+\gamma\right)\eta_{\text{PA}}G_tG_rk}{eKTd^{\alpha}}-e^{-1}\right)+1}{\ln(2)} \tag{13}$$

$$\text{EE}^*=\frac{\text{SE}^*}{\frac{1}{\eta_{\text{PA}}}\frac{KTd^{\alpha}}{G_tG_rk}(2^{\text{SE}^*}-1)+\left(\frac{P_c}{B}+\gamma\right)} \tag{14}$$

Finally, to obtain the optimal values SE^* and EE^* in the SEC model, we need only take $\gamma = 0$.

4. Simulation Results and Discussion

To maintain compliance with 3GPP standards, we have adopted the channel parameters as in [13] and kept them constant throughout this article. These parameters are specified as $\alpha = 3.76$ and $k = 0.0295$ for a carrier frequency of 2 GHz. Likewise, we consider $G_t = 15$ dBi, $G_r = 0$ dBi, $B = 2$ MHz, and $\eta_{\text{PA}} = \frac{1}{3}$.

Figure 1 offers a significant insight into the influence of the distance (d) between the BS and the user on the trade-off between EE and SE. This analysis is based on (7) and is broken down into three distinct scenarios. In the first scenario, RF circuit power (P_{cir}) is zero. The second scenario corresponds to the SEC model, in which the static component of P_{cir} (represented by P_c) is set at 0.1 W. The third scenario involves the SDEC model, with P_{cir} including both a static P_c component of 0.1 W and a dynamic component dependent on the parameter γ, fixed at 10^{-6} W/Hz.

Note that when P_{cir} is zero, EE decreases monotonically as SE increases. In contrast, for the SEC and SDEC models, where P_{cir} is nonzero, EE exhibits convex variation with respect to SE. More precisely, EE increases when $\text{SE}<\text{SE}^*$ and decreases when $\text{SE}>\text{SE}^*$, illustrating the presence of a global maximum at coordinates $(\text{SE}^*, \text{EE}^*)$, as the optimal point where the best trade-off between EE and SE is reached. A comparison between this optimal trade-off point obtained numerically in the SEC and SDEC cases and the analytical equivalent, represented by an enlarged, unfilled symbol, reveals a strong similarity between the optimal values of EE^* and SE^*, irrespective of the distance d considered. Finally, examining the influence of distance on this

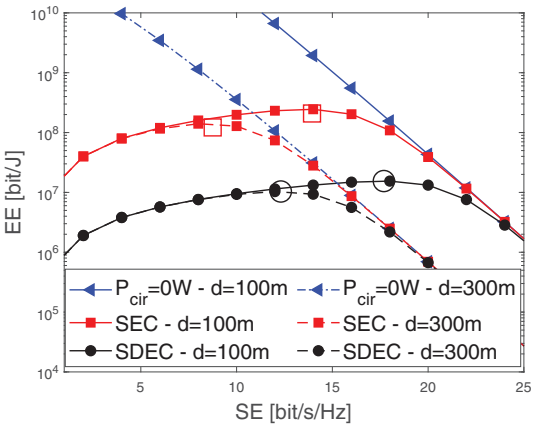

Figure 1. EE as a function of SE and analytically obtained optimal trade-off represented by an enlarged, unfilled symbol for the SEC (for $P_c = 0.1$ W) and SDEC (for $P_c = 0.1$ W and $\gamma = 10^{-6}$ W/Hz) models, with two distance values ($d = 100$ m and 300 m).

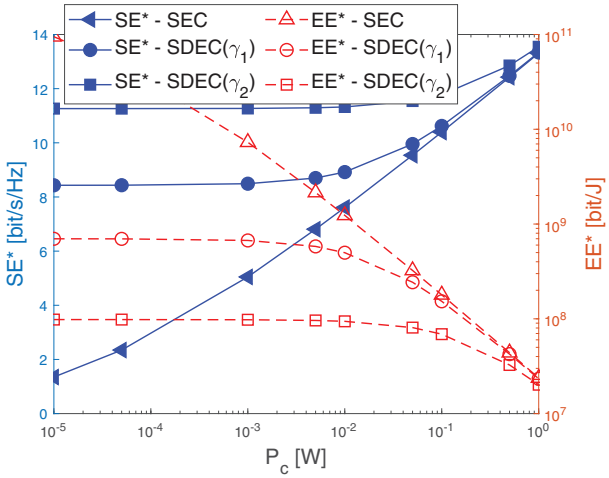

Figure 2. Analytical values of EE and SE as a function of static circuit power P_c for $d = 200$ m, with the SEC model ($\gamma = 0$) and the SDEC model ($\gamma_1 = 10^{-8}$ W/Hz and $\gamma_2 = 10^{-7}$ W/Hz).

optimal trade-off, we find that both SE and EE decrease with increasing d. This variation results from the increase in energy consumed for transmission, noted E'_b (5) with distance, thus leading to an increase in total energy $E_{b,\text{tot}}$ (4), and in other words, a reduction in EE (7). By increasing the value of d, we favor a predominance of E'_b over E_{cir}. Consequently, the reduction in $E_{b,\text{tot}}$ approaching the value of E'_b generates a reduction in SE.

Let us now proceed to an in-depth evaluation of the impact of circuit power (P_{cir}) on the optimal trade-off between EE and SE, which we have analytically determined, focusing on the SEC and SDEC models. This analysis aims to determine how the static component (represented by P_c) and the dynamic part (characterized by the coefficient γ) influence this optimal trade-off.

Having evaluated EE as a function of SE for a constant value of P_c and γ in Figure 1 and having identified the optimal operating point (SE,* EE*), the main objective is to determine SE* and EE* over a wider range of SEC and SDEC model parameter variations. To achieve this aim, the approach is to analytically establish SE* and EE* as a function of the static consumption of the circuits (P_c), as illustrated in Figure 2. This analysis encompasses a range from 0.01 mW to 1 W for both SEC and SDEC models and considers two values of the γ coefficient ($\gamma_1 = 10^{-8}$ W/Hz and $\gamma_2 = 10^{-7}$ W/Hz) in the SDEC mode. Furthermore, to assess the sensitivity of SE* and EE* to variations in the γ coefficient for the SDEC model, we vary its value from 10^{-11} W/Hz to 10^{-5} W/Hz, as illustrated in Figure 3. All the analyses in Figure 3 are carried out, while maintaining a fixed distance d of 200 m and considering two values of static circuit power ($P_c = 0.1$ W and 1 W).

Figures 2 and 3 explicitly demonstrate that an increase in P_c or γ systematically leads to an increase in SE*, accompanied by a concomitant reduction in EE*. This relationship stems from the fact that E_{cir} increases proportionally to the increase in γ or P_c, which, in turn, induces an increase in $E_{b,\text{tot}}$, and, consequently, a decrease in EE. Our main objective, aimed at minimizing $E_{b,\text{tot}}$ (in other words, optimizing EE), tends to approach the value of E_{cir} due to the latter's predominance over E'_b, which ultimately results in an improvement in SE*.

Looking at Figure 2, it is also remarkable that the variability of SE* and EE* progressively increases with increasing P_c in the SDEC model (for both values of γ), asymptotically converging toward the limits of the SEC model. Looking at the P_c limit for the SDEC model, we see that SE* and EE* remain relatively stable below a value of P_c equal to 0.01 W. Above this threshold, these curves show significant variations, converging toward values similar to those of the SEC model. This convergence is explained by the predominant weight of the static part P_c compared with the dynamic part, thus

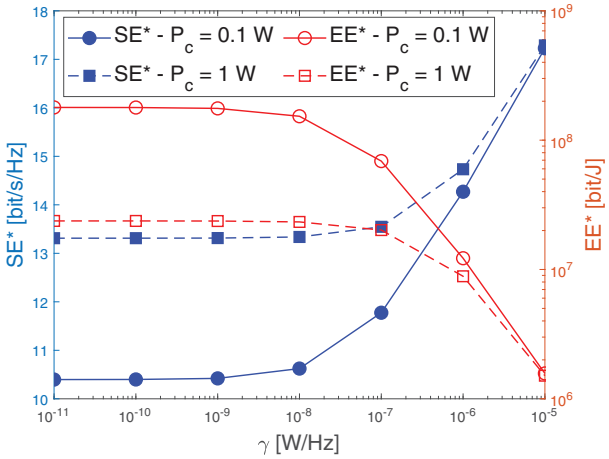

Figure 3. Analytical values of EE and SE as a function of the SDEC model parameter γ, for a distance d of 200 m and two values of static circuit power ($P_c = 0.1$ W and 1 W).

reducing the impact of the γ parameter in the SDEC model compared with the SEC model.

Furthermore, examination of Figure 3 reveals that for both static circuit power levels P_c in the SDEC model, a critical value of the parameter γ lies at γ equal to 10^{-8} W/Hz, beyond which SE^* and EE^* show substantial variations, eventually converging to similar values. This convergence can be attributed to the predominance of the dynamic part over the static part, reducing the influence of P_c when γ has a high value in the SDEC model.

5. Conclusion

This article has conducted an in-depth analysis of the fundamental trade-off between SE and EE in the context of small cell 5G communications, focusing on short-range scenarios. The article proposed both a numerical and analytical optimization solution. In addition, it examined in detail the influence of two distinct RF circuit energy consumption models, namely, the SEC model and the SDEC model. This evaluation is based on analytical equations that describe how optimal SE and EE values withstand extensive variations in the static and dynamic parameters associated with these models. In all, this study offers a significant contribution, shedding light on the challenges and opportunities associated with the optimization of small cell 5G networks, by adopting a holistic perspective that encompasses both EE and SE, while considering the peculiarities of the SEC and SDEC models.

6. References

1. J. Tanveer, A. Haider, R. Ali, and A. Kim, "An Overview of Reinforcement Learning Algorithms for Handover Management in 5G Ultra-Dense Small Cell Networks," *Applied Sciences*, **12**, 1, January 2022, p. 426.
2. M. Younes and Y. Louet, "Comparison of the Transmission Modes of 5G Networks With a High Density of Base Stations Distributed According to Poisson Point Process," 2022 3rd URSI Atlantic and Asia Pacific Radio Science Meeting, Gran Canaria, Spain, May 30–June 4, 2022, pp. 1-4.
3. G. Bacci, E. V. Belmega, P. Mertikopoulos, and L. Sanguinetti, "Energy-Aware Competitive Power Allocation in Heterogeneous Networks With QoS Constraints," *IEEE Transactions on Wireless Communications*, **14**, 9, September 2015, pp. 4728-4742.
4. M. Younes and Y. Louet, "Analysis of Unicast/Broadcast Switch Over with Regard to Resource Allocation for Future Cellular Networks," 2022 4th Global Power, Energy and Communication Conference, Cappadocia, Turkey, June 14–17, 2022, pp. 605-610.
5. M. Sinaie, A. Zappone, E. Jorswieck, and P. Azmi, "A Novel Power Consumption Model for Effective Energy Efficiency in Wireless Networks," *IEEE Wireless Communications Letters*, **5**, 2, December 2016, pp. 152-155.
6. M. Moretti, L. Sanguinetti, and X. Wang, "Resource Allocation for Power Minimization in the Downlink of THP-Based Spatial Multiplexing MIMO-OFDMA Systems," *IEEE Transactions on Vehicular Technology*, **64**, 1, January 2015, pp. 405-411.
7. M. Younes and Y. Louet, "Optimal Density of Base Stations in Dense Networks From the Point of View of Energy Efficiency," *URSI Radio Science Letters*, **4**, November 2022, https://doi.org/10.46620/22-0010.
8. M. Younes and Y. Louet, "Optimizing Energy Efficiency in 5G Small Cell Networks: An Approach Focused on Regulating Power Consumption Related to Transmission and RF Circuits," 2023 35th URSI General Assembly and Scientific Symposium, Sapporo, Japan, August 19–26, 2023, pp. 1-4.
9. S. Cui, A. J. Goldsmith, and A. Bahai, "Energy-Constrained Modulation Optimization," *IEEE Transactions on Wireless Communications*, **4**, 5, September 2005, pp. 2349-2360.
10. C. Diouf, M. Younes, A. Noaja, S. Azou, M. Telescu, et al., "Robustness Analysis of a Parallel Two-Boxes digital Polynomial Predistorter for an SOA-Based CO-OFDM System," *Optics Communications*, **402**, November 2017, pp. 442-452.
11. M. Younes, M. Telescu, N. Tanguy, C. Diouf, P. Morel, et al., "Robustness Improvement of Compact Predistorters in a CO-OFDM System Using Semiconductor Optical Amplifiers," 2017 29th IEEE International Conference on Microelectronics, Beirut, Lebanon, December 10–13, 2017, pp. 1-4.
12. J. E. Sime, P. Morel, M. Younes, I. S. Stievano, M. Telescu, et al., "The Effects of Digital Predistortion in a CO-OFDM System—A Stochastic Approach," *IEEE Photonics Technology Letters*, **32**, 13, July 2020, pp. 763-766.
13. 3rd Generation Partnership Project, *Evolved Universal Terrestrial Radio Access (E-UTRA); Radio Frequency (RF) System Scenarios*, Technical Report 36.942, version 15.0.0, 3GPP, 2018.
14. I. P. Chochliouros, M. A. Kourtis, A. S. Spiliopoulou, P. Lazaridis, Z. Zaharis, et al., "Energy Efficiency Concerns and Trends in Future 5G Network Infrastructures," *Energies*, **14**, 17, August 2021, p. 5392.